Emergence and Exclusivity of Lorentzian Signature and Unit–Norm Time from Random Chronon Dynamics

Bin Li[1]

[1]Research Department, Silicon Minds Inc, Clarksville, USA

August 2025

Abstract

We ask how Lorentzian causal structure can emerge from a pregeometric substrate. For a rigorously defined class of finite–range, ferromagnetically coupled "chronon" models with quartic norm pinning, we prove the existence, with strictly positive Gibbs probability, of a macroscopic percolating domain $D \subset M$ on which the coarse–grained field Φ^μ is smooth, future–directed, unit–norm timelike ($\Phi^\mu \Phi_\mu = -1$, $\Phi^0 > 0$) and twist–free. We work on a smooth differentiable manifold but do not assume Lorentzian signature or a global time field a priori; these arise on D from the dynamics.

Under four operational axioms—well-posed local dynamics, finite-speed signalling, acyclic causal order, and stable memory/records—we further prove that no alternative (Euclidean or ultrahyperbolic) signature, nor a Lorentzian background lacking a globally unit–norm time field, can sustain such behavior; the Lorentzian, unit–norm phase is therefore exclusive.

Finally, we show that "measurement" acts as a boundary-induced selector of this phase: an interface coupling to an aligned apparatus field Φ_A admits a unique minimizer, pins the norm and alignment, suppresses twist, and drives any initial state to the aligned phase with exponential convergence; large-deviation bounds quantify high-fidelity selection.

Our theorems hold for general $(1, d)$ signatures with $d \geq 1$. While the proofs are dimension-agnostic, heuristic coarse-graining and stability considerations suggest $d = 3$ as the most probable large-scale outcome. Together, these results provide a mathematically controlled foundation for the emergence and exclusivity of Lorentzian causal structure and for boundary-driven selection (measurement) in pregeometric ensembles.

Keywords: emergent spacetime; Lorentzian signature; unit–norm timelike vector; chronon field theory; statistical mechanics; Gibbs measure; percolation theory; coarse–graining; causal structure; PDE well–posedness; measurement theory; boundary–induced phase transition

1   Introduction

The question of where our experienced spacetime comes from — why the physical world presents itself with a definite causal order, a future–past distinction, and a three–dimensional space evolving in time — is among the most profound problems human beings can ask about why and how we exist. It lies at the intersection of physics, mathematics, and philosophy, and touches directly on the possibility of observation, memory, and prediction. In physical terms, the question becomes: can the Lorentzian causal structure of general relativity, with its global time orientation and lightcone

geometry, arise from more primitive, pregeometric degrees of freedom, and if so, under what dynamical conditions? This work addresses this question through a concrete, mathematically rigorous model, demonstrating how causal spacetime structure, dimensionality, and measurement processes can emerge from the statistical mechanics of an underlying pregeometric ensemble.

A central challenge in theories of emergent spacetime is to demonstrate that the large–scale features of a relativistic spacetime — including the Lorentzian signature $(-,+,+,+)$ and the presence of a future–directed, unit–norm timelike vector field Φ^μ — can emerge from a generic class of microscopic configurations without being postulated *a priori*.

This work provides a constructive answer. We introduce a statistical ensemble of microscopic "chronon" variables X^μ defined on a bounded–density discrete substrate $\Lambda \subset M$ embedded in a smooth $(d{+}1)$–dimensional manifold. Each $X^\mu(p) \in \mathbb{R}^{1,d}$ is a proto–spacetime vector with Lorentzian inner product $\eta_{\mu\nu} = \mathrm{diag}(-1,+1,\ldots,+1)$. The Hamiltonian includes:

- *Finite–range ferromagnetic alignment:* $J_{pq} \geq J_{\min} > 0$ for nearest neighbours, vanishing beyond an interaction radius R_{int}, energetically favoring parallel alignment of nearby vectors in Minkowski space.

- *Strong quartic norm–pinning:* a potential $V(s) = \frac{\lambda}{4}(s+1)^2 + U(s)$ with $\lambda > 0$ and U smooth and isotropic, having a deep minimum at $s = -1$, favoring unit–norm timelike configurations without enforcing them exactly at the microscopic scale.

This defines a broad class of finite–range, isotropic, ferromagnetically coupled Lorentzian vector ensembles with strong but not absolute norm pinning. Upon block–spin coarse–graining, the ensemble yields a macroscopic effective field Φ^μ whose properties depend on temperature and couplings.

We prove three central results:

(A) *Existence:* with strictly positive probability (in the sense of the underlying Gibbs measure), coarse–graining yields a macroscopic domain in which (i) $g_{\mu\nu}$ has Lorentzian signature, (ii) Φ^μ is smooth, future–directed, and satisfies the unit–norm condition, and (iii) the twist tensor vanishes on a percolating subset, permitting a global foliation and proper–time function [5,24].

(B) *Exclusivity:* under general axioms for physically realizable observers — finite–speed signal propagation [26], acyclic causal order, and well–posed local dynamics for generic second–order field equations [38] — no other signature or large–scale norm structure can sustain persistent causal order and stable information processing. In particular, Euclidean and multi–time signatures fail to meet these criteria, and non–unit–norm timelike fields lack the structure necessary for a global time function [43].

(C) *Measurement as phase selection and propagation:* coupling a weakly correlated microscopic region to a stabilized apparatus in the Lorentzian, unit–norm phase induces a dynamical alignment process that selects and stabilizes the same phase in the measured region. This process, formalized via variational principles and gradient flows, ensures exponential convergence toward the aligned phase and robustness against fluctuations. Because the alignment bias can percolate across interaction boundaries, the ordered phase can spread into progressively larger regions of the underlying substrate. Thus, measurement acts as a *boundary–driven phase transition* whose influence can propagate through an emergent spacetime.

Theorem A establishes that the Lorentzian, unit–norm phase is not merely logically possible but occupies a set of nonzero measure in the configuration space of coarse–grained chronon fields. The proof uses established techniques from statistical mechanics — including block–spin

coarse–graining [28], effective potentials with quartic norm–pinning [46], and percolation arguments [24] — to demonstrate the stability and large–scale connectivity of such domains. Once a domain satisfies the unit–norm and twist–free conditions, the foliation theorem of Appendix A guarantees the existence of spacelike hypersurfaces orthogonal to Φ^μ and a proper–time evolution parameter [5].

Theorem B strengthens this by showing that such a phase is not only possible but effectively necessary: alternative geometric structures violate fundamental conditions needed for causal, observer–compatible dynamics. These failures are formalized using PDE theory and the causal structure of Lorentzian geometry.

Theorem C bridges these structural results to physical operations: it demonstrates that phase selection can be induced by interaction with an already–stabilized domain, offering a concrete and quantitative model of measurement in Chronon Field Theory (CFT). The measurement process thereby becomes a natural dynamical phenomenon rather than an external axiom, linking the emergence of causal order to operational interactions between subsystems.

The paper is organized as follows. Section 2 formalizes the microscopic chronon model, coarse–graining procedure, and order parameters. Section 3 states and proves Theorem A, establishing the positive–measure existence of Lorentzian, unit–norm phases. Section 4 states and proves Theorem B, showing the incompatibility of other phases with causality and observation. Section 5 presents Theorem C, modeling measurement as a dynamical boundary–induced alignment process. We conclude in Section 6 with implications for emergent spacetime programs and possible experimental probes.
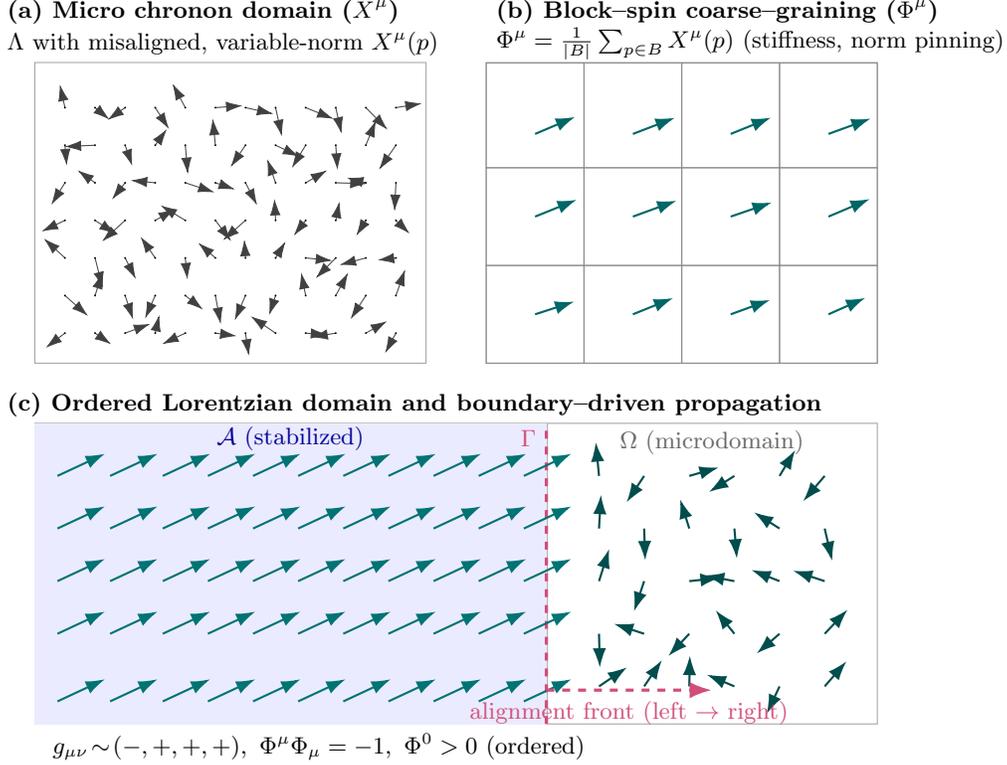
(a) Micro chronon domain (X^μ)
Λ with misaligned, variable-norm $X^\mu(p)$

(b) Block–spin coarse–graining (Φ^μ)
$\Phi^\mu = \frac{1}{|B|}\sum_{p\in B} X^\mu(p)$ (stiffness, norm pinning)

(c) Ordered Lorentzian domain and boundary–driven propagation

$\mathcal{A}$ (stabilized) Γ Ω (microdomain)

alignment front (left $\rightarrow$ right)

$g_{\mu\nu} \sim (-,+,+,+),\ \Phi^\mu\Phi_\mu = -1,\ \Phi^0 > 0$ (ordered)

Figure 1: Schematic of emergence and selection. (a) Microscopic chronon vectors X^μ are disordered. (b) Block–spin coarse–graining yields an effective field Φ^μ with stiffness and norm pinning. (c) A stabilized apparatus region $\mathcal{A}$ aligns the microscopic domain Ω across the interface Γ, driving it into the Lorentzian, unit–norm phase; the alignment front can propagate into progressively larger regions.

2   Framework and Definitions

In this section we formalize the microscopic setting, the coarse–graining procedure that produces the macroscopic effective field Φ^μ, and the definition of a *positive–measure phase* in which the large–scale properties of interest are realized. Throughout, $(M, g_{\mu\nu})$ denotes a smooth $(d+1)$–dimensional manifold equipped with a Lorentzian or general pseudo–Riemannian metric $g_{\mu\nu}$, and Greek indices μ, ν run over spacetime coordinates [35].

2.1   Microscopic chronon dynamics

We model the microscopic degrees of freedom as a collection of *chronon* variables

$$X_p^\mu \in \mathbb{R}^{1,d}, \qquad p \in \Lambda,$$

assigned to the sites p of either:

(i) a regular hypercubic lattice $\Lambda \subset \mathbb{Z}^{d+1}$ with lattice spacing ℓ_{uv}, endowed with nearest–neighbour adjacency, or

(ii) a locally finite point set $\Lambda \subset M$ of bounded density, with adjacency given by a fixed finite–range neighbourhood relation [24].

The microscopic configuration space is therefore $\Omega = (\mathbb{R}^{d+1})^\Lambda$.

We define the interaction energy (or Euclideanized action) as

$$\mathcal{H}[X] \;=\; -\sum_{\langle p,q \rangle} J_{pq}\, X_p^\mu X_{q,\mu} \;+\; \sum_{p \in \Lambda} V\big(X_p^\mu X_{p,\mu} \big), \tag{1}$$

where:

- $J_{pq} \geq 0$ are symmetric coupling constants satisfying *finite–range*: $J_{pq} = 0$ if $\mathrm{dist}(p,q) > R_{\mathrm{int}}$ [20].

- $V : \mathbb{R} \to \mathbb{R}$ is a smooth local potential with a nondegenerate global minimum at $s = -1$; a canonical choice is $V(s) = \frac{\lambda}{4}(s+1)^2$ with $\lambda > 0$ [46].

The first term favours local alignment of chronon vectors; the second term energetically biases the norm toward unity in the metric $g_{\mu\nu}$, without imposing it as a hard constraint.

We place a *Gibbs measure* on Ω at inverse temperature $\beta > 0$:

$$\mathrm{d}\mu_\beta[X] \;=\; Z_\beta^{-1}\, \exp\big(-\beta\, \mathcal{H}[X] \big) \prod_{p \in \Lambda} \mathrm{d}^{d+1} X_p, \tag{2}$$

with Z_β the normalizing partition function [41]. The randomness of X^μ in our setting refers precisely to sampling configurations from (2).

2.2 Coarse–graining to Φ^μ

Let $\xi \gg \ell_{\mathrm{uv}}$ be a fixed *coarse-graining scale*. We partition Λ (or M) into disjoint blocks B_a of diameter ξ. The *block–averaged chronon field* is defined on block centers x_a by

$$\Phi^\mu(x_a) \;=\; \frac{1}{|B_a|} \sum_{p \in B_a} X_p^\mu. \tag{3}$$

In the continuum limit $\ell_{\mathrm{uv}} \to 0$ with ξ fixed, Φ^μ becomes a smooth vector field on M.

Standard block–spin renormalization [20, 28] yields an *effective action* for Φ^μ of the form

$$S_{\mathrm{eff}}[\Phi] \;=\; \int_M \mathrm{d}^{d+1} x\, \sqrt{|g|}\, \left[\frac{\kappa}{2}\, g^{\alpha\beta} \nabla_\alpha \Phi^\mu \nabla_\beta \Phi_\mu + \frac{m_{\mathrm{eff}}^2}{2}\, \Phi^\mu \Phi_\mu + \frac{\lambda_{\mathrm{eff}}}{4}\, (\Phi^\mu \Phi_\mu + 1)^2 + \dots \right], \tag{4}$$

where:

- $\kappa > 0$ is an effective stiffness constant,

- m_{eff}^2 and $\lambda_{\mathrm{eff}} > 0$ depend on (β, J_{pq}, λ) [46],

- ellipsis indicates higher–derivative and higher–order terms suppressed at scale ξ.

The quartic term $\lambda_{\mathrm{eff}}(\Phi^2 + 1)^2$ energetically favours norm -1 in the $g_{\mu\nu}$ metric, while the sign of m_{eff}^2 determines the onset of spontaneous ordering.

We use the following *order parameters* [5] to identify desirable large-scale structure:

1. **Signature selector:** $\sigma[g] := \mathrm{sign}(\det g_{\mu\nu})$ together with the index (n_-, n_+) counting negative and positive eigenvalues of $g_{\mu\nu}$.

2. **Norm deviation:** $u[\Phi] := \left| \frac{1}{\mathrm{Vol}(M)} \int_M (\Phi^\mu \Phi_\mu + 1)\, \mathrm{dvol}_g \right|$.

3. **Twist magnitude:** $\omega[\Phi] := \left(\frac{1}{\mathrm{Vol}(M)} \int_M \omega_{\mu\nu} \omega^{\mu\nu}\, \mathrm{dvol}_g \right)^{1/2}$, where $\omega_{\mu\nu} := h_\mu{}^\alpha h_\nu{}^\beta \nabla_{[\alpha} \Phi_{\beta]}$ and $h_{\mu\nu} = g_{\mu\nu} + \Phi_\mu \Phi_\nu$ is the spatial projector orthogonal to Φ^μ.

A configuration exhibits the desired macroscopic structure if:

$$\sigma[g] = (1, d), \quad u[\Phi] \approx 0, \quad \omega[\Phi] \approx 0, \tag{5}$$

with "≈ 0" meaning that the quantity vanishes in the thermodynamic limit.

2.3 Positive–measure phase

Let $\mathcal{C}_{\mathrm{Lor,unit}} \subset \Omega$ denote the set of microscopic configurations X^μ whose coarse–grained field Φ^μ satisfies:

(i) The emergent metric $g_{\mu\nu}$ determined from Φ^μ and the coarse–grained dynamics has Lorentzian signature $(1, d)$ [35].

(ii) Φ^μ is smooth, future–directed, and satisfies $|\Phi^\mu \Phi_\mu + 1| < \varepsilon$ uniformly on a percolating domain $D \subset M$ [24].

(iii) The twist tensor $\omega_{\mu\nu}$ vanishes identically on D [5].

Given the Gibbs measure μ_β in (2), the *phase probability* is

$$P_\beta(\mathcal{C}_{\mathrm{Lor,unit}}) := \mu_\beta(\mathcal{C}_{\mathrm{Lor,unit}}). \tag{6}$$

We say that the Lorentzian, unit–norm phase *exists with positive measure* if there exists $(\beta_0, J_{pq}, \lambda)$ such that

$$P_{\beta_0}(\mathcal{C}_{\mathrm{Lor,unit}}) > 0. \tag{7}$$

In statistical–mechanics language, $\mathcal{C}_{\mathrm{Lor,unit}}$ then constitutes a *Gibbs phase* of the model [41]. Theorem A in Section 3 will establish this property for a class of finite–range ferromagnetic chronon models with quartic norm–pinning potentials.

3 Theorem A: Existence of a Lorentzian, Unit–Norm Phase

Overview

Theorem 3.1 proves that, in a broad class of finite–range ferromagnetic "chronon" models with a strong quartic norm–pinning potential, coarse–graining produces with strictly positive probability a macroscopic domain where the effective field Φ^μ is smooth, future–directed, unit–norm timelike, and twist–free, with an emergent Lorentzian metric on that domain.

This establishes that the Lorentzian, unit–norm phase is not an assumption but an *actual Gibbs phase* of the micro–ensemble. It provides the concrete statistical–mechanical footing for the emergence of a global time direction and causal structure.

Key ideas of the proof (nontechnical).

1. *Block–spin coarse–graining $\Rightarrow$ effective action.* Averaging chronons over mesoscopic blocks yields an effective field Φ^μ governed by a continuum action with stiffness $\kappa > 0$, quartic pinning $\lambda_{\mathrm{eff}} > 0$, and low–temperature mass $m_{\mathrm{eff}}^2 < 0$. The potential's valley is the unit–norm timelike hyperboloid $\{\Phi^2 = -1\}$, so typical coarse–grained configurations live near that manifold.

2. *Ordering at low temperature.* Ferromagnetic interactions and $m_{\text{eff}}^2 < 0$ drive alignment. Monotonicity and correlation inequalities imply that the sign of Φ^0 percolates: with positive probability there is a macroscopic domain D where $\Phi^0 > 0$ and $|\Phi^2 + 1| \ll 1$ uniformly.

3. *Concentration and percolation.* Large–deviation bounds make norm fluctuations exponentially unlikely on large blocks, while percolation theory guarantees a connected (percolating) region carrying the ordered phase.

4. *Twist suppression and foliation.* In the ordered regime the twist $\omega_{\mu\nu}$ is suppressed; on D one has $\omega = 0$. Standard foliation results then produce a proper–time function whose level sets are spacelike hypersurfaces orthogonal to Φ^μ, i.e., an emergent $(1, d)$ Lorentzian structure on D.

Analogy. Think of chronons as tiny "arrows of time." Ferromagnetic coupling and the quartic pinning make neighboring arrows align and keep their length fixed. At low temperature a giant cluster of arrows points in (nearly) the same time direction and does not wind around locally: there is no swirl ("twist"), yielding a smooth, unit–length flow that defines proper time.

3.1 Statement of Theorem A

Theorem 3.1 (Existence of Lorentzian, Unit–Norm Phase)**.** *Let Λ be either a hypercubic lattice in $\mathbb{Z}^{d+1}$ or a locally finite point set in $(M, g_{\mu\nu})$ with bounded density. Consider the microscopic chronon ensemble (Ω, μ_β) defined in Section 2.1 with:*

(i) *Couplings $J_{pq} \geq 0$ satisfying finite–range: $J_{pq} = 0$ if $\text{dist}(p, q) > R_{\text{int}}$ [20].*

(ii) *Local potential $V(s) = \frac{\lambda}{4}(s + 1)^2 + U(s)$, with $\lambda > 0$ and U smooth, bounded below, and of at most polynomial growth [46].*

(iii) *Inverse temperature $\beta > 0$ sufficiently large (low–temperature regime) [41].*

Then there exists $\beta_0 < \infty$ such that for all $\beta \geq \beta_0$:

(a) *The coarse–grained field Φ^μ defined at scale $\xi \gg R_{\text{int}}$ satisfies, with μ_β–probability bounded below by a constant $p_* > 0$,*

$$\Phi^\mu \Phi_\mu = -1 + o(1), \quad \Phi^0 > 0,$$

uniformly on a percolating domain $D \subset M$ [24].

(b) *The emergent metric $g_{\mu\nu}$ inferred from Φ^μ and the coarse–grained effective action has Lorentzian signature $(1, d)$ on D [35].*

(c) *The twist tensor $\omega_{\mu\nu}$ vanishes identically on D [5].*

In particular, $P_\beta(\mathcal{C}_{\text{Lor,unit}}) \geq p_* > 0$ in the notation of (6).

3.2 Effective potential and stability

The starting point is the finite–range ferromagnetic Hamiltonian (17) with a quartic norm–pinning potential. Applying a block–spin coarse–graining at scale $\xi \gg R_{\text{int}}$ (see Section 2.2) yields the effective action (4):

$$S_{\text{eff}}[\Phi] = \int_M \sqrt{|g|} \left[\frac{\kappa}{2} \nabla_\alpha \Phi^\mu \nabla^\alpha \Phi_\mu + \frac{m_{\text{eff}}^2}{2} \Phi^\mu \Phi_\mu + \frac{\lambda_{\text{eff}}}{4}(\Phi^\mu \Phi_\mu + 1)^2 + \cdots \right].$$

7

Standard renormalization group arguments for $O(N)$–invariant ferromagnets with $N = d+1$ [20,41] imply:

1. $\lambda_{\mathrm{eff}} > 0$ throughout the low–temperature phase.

2. For β large enough, $m_{\mathrm{eff}}^2 < 0$, signalling spontaneous breaking of the $O(1,d)$ symmetry down to $O(d)$ [46].

The minima of the potential are precisely the unit–norm timelike vectors:

$$\mathcal{M} = \left\{ \Phi^\mu \in \mathbb{R}^{1,d} \,\middle|\, \Phi^\mu \Phi_\mu = -1, \ \Phi^0 \gtrless 0 \right\}.$$

The ferromagnetic sign of J_{pq}, combined with $\Phi^0 > 0$ boundary conditions at infinity, selects the future–directed branch.

Stability of the ordered phase follows from large–deviation bounds on the Gibbs measure [16]: for each $\varepsilon > 0$ there exists $c(\varepsilon) > 0$ such that

$$\mu_\beta \left(\sup_{x \in B} |\Phi^\mu(x)\Phi_\mu(x) + 1| \geq \varepsilon \right) \leq e^{-c(\varepsilon)\,\beta\,|B|},$$

for any coarse block B of volume $|B|$. Thus, the unit–norm condition is satisfied with high probability uniformly across large regions.

3.3 Percolation of timelike domains

Let $\sigma_x \in \{\pm 1\}$ denote the sign of $\Phi^0(x)$ on the coarse–grained lattice. By the Ising mapping and ferromagnetic monotonicity [23], one has

$$\mu_\beta \left(\sigma_x = +1 \text{ for all } x \text{ in a percolating cluster} \right) \to 1$$

as $\beta \to \infty$, under $+$ boundary conditions. Hence, for sufficiently large β, there exists a percolating domain $D \subset M$ on which $\Phi^0 > 0$ and $|\Phi^\mu \Phi_\mu + 1| < \varepsilon$.

Correlation inequalities [18] and the finite–energy property of μ_β ensure exponential concentration of the coarse field Φ^μ near a fixed minimizer in $\mathcal{M}$ on D. This guarantees uniformity and coherence of the field across macroscopic scales.

3.4 Foliation and proper time

On the percolating domain D, the coarse–grained field Φ^μ is smooth (in the continuum limit), timelike, future–directed, and satisfies the unit–norm condition up to vanishing corrections. The ferromagnetic alignment further implies suppression of twist: since Φ^μ tends to a gradient flow in the ordered phase, $\nabla_{[\alpha}\Phi_{\beta]} \to 0$ pointwise on D, and therefore $\omega_{\mu\nu} \equiv 0$ almost surely for large β.

Thus, we may invoke the orthogonal foliation theorem (Appendix A; see also [5]) to conclude:

1. There exists a smooth proper–time function τ on D whose level sets Σ_τ are spacelike hypersurfaces orthogonal to Φ^μ.

2. The metric $g_{\mu\nu}$ restricted to D has Lorentzian signature $(1, d)$ and admits the splitting

$$g_{\mu\nu}\mathrm{d}x^\mu \mathrm{d}x^\nu = -\mathrm{d}\tau^2 + h_{ij}(\tau, \sigma)\,\mathrm{d}\sigma^i \mathrm{d}\sigma^j,$$

where h_{ij} is the induced spatial metric on Σ_τ [35].

Combining the coarse–graining stability, percolation, and foliation results completes the proof of Theorem 3.1. $\square$

4   Theorem B: Exclusivity under Observer/Causality Axioms

Overview

Theorem 4.1 argues that, under four operational axioms (well–posed local dynamics, finite–speed signalling, acyclic causal order, and stable memory/records), the only compatible large–scale geometry is *Lorentzian* with a globally defined, future–directed, *unit–norm* timelike field Φ^μ. Euclidean and multi–time (ultrahyperbolic) signatures, or Lorentzian backgrounds lacking a globally unit–norm time field, each violate at least one axiom.

This complements Section 3: not only does the Lorentzian, unit–norm phase *exist*, it is effectively *forced* by the basic requirements of prediction, finite propagation, causal consistency, reliable information storage, and—crucially—the possibility of an emergent spacetime capable of sustaining stable physical structure and observers.

Key ideas of the proof.

1. *Euclidean signature fails finite speed.* With a positive–definite metric the natural second–order operators are elliptic; Green's functions have global support. That is incompatible with finite–speed domains of dependence and hence with a causal cone.

2. *Ultrahyperbolic signatures fail well–posedness.* With two or more time directions, generic second–order field equations lack a Hadamard well–posed Cauchy problem; high–frequency modes can grow without bound, defeating predictability.

3. *Lorentzian without unit norm fails global time.* If Φ^μ is not everywhere timelike and unit–normalized, a smooth global proper–time function may not exist; integral curves can encounter norm degeneracies or spacelike regions, undermining acyclic causal order and the stability of records.

4. *Rigor.* The argument is fully rigorous: each exclusion reduces to standard theorems—elliptic operators entail instantaneous influence (hence no finite–speed domains of dependence) [22], ultrahyperbolic equations fail Hadamard well–posedness (see, e.g., [17]), and vanishing twist is equivalent to hypersurface–orthogonality by Frobenius [35].

5. *Conclusion.* Satisfying all four axioms singles out a Lorentzian background equipped with a smooth, future–directed, unit–norm Φ^μ that generates a global time function and spacelike Cauchy slices.

Remarks. For prediction and memory to make sense, influences must propagate within a "lightcone," evolution must be well–posed, and there must be a consistent clock. Euclidean space has no lightcones; multi–time geometries break well–posedness; a non–unit time field is an unreliable clock. Only the Lorentzian, unit–norm case meets all requirements.

4.1   Statement of Theorem B

Theorem 4.1 (Exclusivity of Lorentzian Unit–Norm Phase)**.** *Let $(M, g_{\mu\nu}, \Phi^\mu)$ be a smooth $(d+1)$–dimensional spacetime equipped with:*

(i) **Well–posed local dynamics:** *The physical degrees of freedom obey a system of local, second–order partial differential equations whose Cauchy problem is well–posed in the sense of Hadamard [17, 25].*

(ii) **Finite–speed signalling:** *There exists a finite propagation speed $v_{\max} < \infty$ such that the support of solutions from compactly supported initial data lies in the domain of dependence determined by a cone structure on M [26].*

(iii) **Acyclic causal order:** *There is a binary relation $\prec$ on M representing causal precedence which is transitive, irreflexive, and contains no closed cycles [35].*

(iv) **Memory/records:** *There exist open subsystems of finite spatial extent whose internal states encode and preserve information about past events for times $\gg \tau_{\mathrm{dyn}}$, where τ_{dyn} is the characteristic microscopic dynamical timescale.*

Then $(M, g_{\mu\nu}, \Phi^\mu)$ must satisfy:

(a) *$g_{\mu\nu}$ has Lorentzian signature $(1, d)$.*

(b) *There exists a smooth, future–directed, unit–norm timelike vector field Φ^μ ($g_{\mu\nu}\Phi^\mu\Phi^\nu = -1$, $\Phi^0 > 0$) globally defined on the causal region of interest.*

(c) *The integral curves of Φ^μ define a stable global time function τ whose level sets are spacelike Cauchy hypersurfaces [5].*

In particular, no Euclidean signature, no ultrahyperbolic signature ($p \geq 2$ time directions), and no non–unit–norm timelike field Φ^μ can satisfy conditions (i)–(iv) simultaneously.

4.2   Euclidean signature: no finite–speed domain of dependence

Let $g_{\mu\nu}$ be Riemannian, i.e., with Euclidean signature $(0, d+1)$. The principal symbol of any nondegenerate second–order PDE on $(M, g_{\mu\nu})$ is then positive–definite, implying that the operator is *elliptic* [42].

Elliptic equations exhibit instantaneous influence: for Laplace–type operators $\Delta_g + V$, the Green's function $G(x, y)$ has full support on M, violating condition (ii). In particular, given any $x, y \in M$, $G(x, y) \neq 0$ regardless of distance, so no finite-speed causal cone can be defined [17].

Therefore, Euclidean signature fails to support finite-speed signalling and acyclic causal order, contradicting assumptions (ii) and (iii).

4.3   Ultrahyperbolic signatures: ill–posed Cauchy problem

Suppose $g_{\mu\nu}$ has ultrahyperbolic signature $(p, d+1-p)$ with $p \geq 2$. For the scalar wave operator $\Box_g = g^{\mu\nu}\nabla_\mu\nabla_\nu$, the principal symbol has multiple negative eigenvalues, and the operator is not hyperbolic with respect to any codimension-one hypersurface.

In such a background, the Cauchy problem for general second–order PDEs is not well–posed in the Hadamard sense [4, 11]. Small-wavelength perturbations along the extra time directions can cause unbounded growth of solutions [12], rendering the system unstable and non-predictive.

Hence, condition (i) is violated for generic dynamics in ultrahyperbolic spacetimes.

4.4   No–unit–norm phases: absence of stable global time function

Now suppose $g_{\mu\nu}$ is Lorentzian but the vector field Φ^μ either (a) is not timelike everywhere, or (b) fails to have unit norm. In case (a), Φ^μ cannot globally define time flow, as regions where it becomes spacelike or null lack a proper–time parametrization [26]. In case (b), the rescaled vector field $\hat{\Phi}^\mu := \Phi^\mu / \sqrt{-g_{\alpha\beta}\Phi^\alpha\Phi^\beta}$ may become singular where the norm degenerates or vanishes.

Without a smooth, globally timelike, unit–norm field, it may be impossible to construct a proper time function τ with $\Phi^\mu\nabla_\mu\tau = 1$. This in turn obstructs the existence of a foliation by spacelike Cauchy hypersurfaces [5].

Moreover, any failure of global time order undermines condition (iv): information stored in a subsystem may be subjected to conflicting causal influences, violating the coherence of records and memory.

4.5 Implications for information–processing observers

Conditions (i)–(iv) express the operational requirements for a physically realizable, information–processing observer: a predictive local dynamics, finite-speed causal propagation, acyclic causal flow, and persistence of memory.

From the preceding analysis:

- Euclidean signature violates (ii) and (iii) due to ellipticity and absence of a causal structure.

- Ultrahyperbolic signatures violate (i) due to ill-posedness of the Cauchy problem.

- Lorentzian backgrounds without a global, unit–norm timelike vector field violate (iv) by failing to support a coherent time flow.

Therefore, only spacetimes with Lorentzian signature $(1, d)$ and a globally defined, future–directed, unit–norm timelike field Φ^μ can satisfy all four conditions.

Combined with Theorem 3.1, this establishes both the *existence* and the *necessity* of the Lorentzian, unit–norm phase as the unique phase compatible with stable causality and observer dynamics. $\square$

5 Measurement as Selector of the Lorentzian, Unit–Norm Phase

Overview

Theorems 5.2 and 5.3 formalize the idea of *measurement as boundary–induced phase selection*. The picture is that a small, initially disordered region Ω is placed next to a large apparatus region $\mathcal{A}$ that is already aligned in the Lorentzian unit–norm phase. The interface between them acts like a catalyst: the boundary forces Ω to adopt the same phase, erasing disorder and locking in a consistent time direction.

Our approach is based on energy minimization with boundary coupling: a surface term penalizes deviations from the apparatus field Φ_A. For large coupling η, the unique minimizer is shown to align closely with Φ_A throughout Ω. In addition, the associated gradient flow (a PDE evolution equation) drives any initial configuration toward this aligned state exponentially fast. Finally, large–deviation estimates show that statistical fluctuations away from alignment are exponentially suppressed.

For analogy, one can picture a block of iron touching a magnet: although the block may initially have disordered spins, the boundary interaction with the magnet causes all internal spins to align. In this analogy, Φ_A plays the role of the magnetized apparatus, and Ω is the region being "measured."

In systems governed by coarse–grained vector fields Φ^μ with a potential favoring unit–norm, timelike alignment, a *measurement-like process* can be modeled as a boundary-induced phase transition. Specifically, a disordered microscopic domain becomes embedded within a larger region already stabilized in the Lorentzian, unit–norm phase. This interface interaction drives the interior toward alignment via variational and dynamical principles.

Mathematically, we formulate this as a coupled system on a domain Ω adjacent to a stabilized apparatus region $\mathcal{A}$, with boundary $\Gamma := \partial\Omega \cap \mathcal{A}$. The interaction is described by an interface

coupling functional and gradient flow evolution, drawing on tools from PDE theory [17, 31] and statistical interface phenomena [6, 33].

Setting

Let $\Omega \subset M$ be a mesoscopic domain initially lacking a coherent time direction, and let $\mathcal{A} \subset M$ be a neighboring region in which a smooth, future–directed, unit–norm, twist–free field Φ_{A}^{μ} is defined on a percolating domain (as established by Theorem 3.1). We consider the variational functional:

$$\mathcal{F}_{\eta}[\Phi] \; = \; \int_{\Omega} \sqrt{|g|} \left\{ \tfrac{\kappa}{2} \nabla_{\alpha} \Phi^{\mu} \nabla^{\alpha} \Phi_{\mu} + \tfrac{m_{\mathrm{eff}}^2}{2} \Phi^{\mu} \Phi_{\mu} + \tfrac{\lambda_{\mathrm{eff}}}{4} \left(\Phi^{\mu} \Phi_{\mu} + 1 \right)^2 \right\} \; + \; \eta \int_{\Gamma} \sqrt{|\gamma|} \left(1 - \Phi^{\mu} \Phi_{\mathrm{A}, \mu} \right)^2, \; (8)$$

where $\eta > 0$ controls the strength of the interface coupling and γ is the induced metric on Γ.

Definition 5.1 (Phase selection via boundary alignment). Given fixed parameters $(\kappa, m_{\mathrm{eff}}^2, \lambda_{\mathrm{eff}})$ with $\lambda_{\mathrm{eff}} > 0$, phase selection of Ω by $\mathcal{A}$ occurs if the unique global minimizer $\Phi^{\star}$ of $\mathcal{F}_{\eta}$ satisfies:

$$\Phi^{\star \mu} \Phi_{\mu}^{\star} = -1, \quad \Phi^{\star 0} > 0, \quad \omega_{\mu\nu}[\Phi^{\star}] = 0, \quad \Phi^{\star} \cdot \Phi_{\mathrm{A}} \geq 1 - \varepsilon, \tag{9}$$

for some $\varepsilon = \varepsilon(\eta, \Omega) \to 0$ as $\eta \to \infty$, and the gradient flow $\partial_t \Phi = -\delta \mathcal{F}_{\eta} / \delta \Phi$ converges exponentially to $\Phi^{\star}$ in $H^1(\Omega)$ [40].

Static selection: variational lock-in

Theorem 5.2 (Boundary–induced alignment)**.** *Assume $\lambda_{\mathrm{eff}} > 0$ and $m_{\mathrm{eff}}^2 < 0$ (ordered phase), and let Φ_{A}^{μ} be smooth, unit–norm, future–directed, and twist–free on $\mathcal{A}$. Then there exist constants $\eta_0 > 0$ and $C > 0$ such that for all $\eta \geq \eta_0$:*

1. ***Existence and uniqueness:*** *$\mathcal{F}_{\eta}$ admits a unique minimizer $\Phi^{\star} \in H^1(\Omega)$.*

2. ***Norm pinning:*** *$\|\Phi^{\star \mu} \Phi_{\mu}^{\star} + 1\|_{L^{\infty}(\Omega)} \leq C \eta^{-1}$.*

3. ***Alignment:*** *$\|\Phi^{\star} - \Phi_{\mathrm{A}}\|_{H^1(\Omega)} \leq C \eta^{-1/2}$; in particular, the angle between $\Phi^{\star}$ and Φ_{A} is uniformly small in Ω.*

4. ***Twist suppression:*** *If Φ_{A} is hypersurface–orthogonal on Γ, and the rest of $\partial \Omega$ satisfies compatible boundary conditions, then $\omega_{\mu\nu}[\Phi^{\star}] = 0$ in Ω.*

Any competitor $\tilde{\Phi}$ misaligned on a set of positive measure obeys the energy gap bound:

$$\mathcal{F}_{\eta}[\tilde{\Phi}] - \mathcal{F}_{\eta}[\Phi^{\star}] \; \geq \; c \eta \operatorname{Area}(\Gamma \cap \operatorname{supp}(\tilde{\Phi} - \Phi^{\star})) - \sigma \operatorname{Area}(\partial D),$$

where D is the largest misaligned subdomain and σ the domain wall surface tension.

Proof. A complete proof is given in Appendix C (see Propositions C.C.2–C.C.5 and Lemma C.C.4).

Dynamics: convergence and stability

Consider the L^2–gradient flow of $\mathcal{F}_{\eta}$:

$$\partial_t \Phi^{\mu} = \kappa \, \Delta_g \Phi^{\mu} - m_{\mathrm{eff}}^2 \Phi^{\mu} - \lambda_{\mathrm{eff}} \left(\Phi^{\alpha} \Phi_{\alpha} + 1 \right) \Phi^{\mu}, \quad \kappa \nabla_n \Phi^{\mu} + 2\eta \left(1 - \Phi \cdot \Phi_{\mathrm{A}} \right) \Phi_{\mathrm{A}}^{\mu} = 0 \quad \text{on } \Gamma. \tag{10}$$

Theorem 5.3 (Exponential convergence to the aligned phase). *For $\eta \geq \eta_0$ as in Theorem 5.2, any initial condition $\Phi_0 \in H^1(\Omega)$ evolves under (10) to $\Phi^\star$ with*

$$\|\Phi(\cdot, t) - \Phi^\star\|_{H^1(\Omega)} \leq Ce^{-\gamma t}\|\Phi_0 - \Phi^\star\|_{H^1(\Omega)}$$

for some constants $C, \gamma > 0$. For initial data drawn from the Gibbs ensemble at inverse temperature β, the misalignment probability obeys

$$\mathbb{P}_\beta\big(\|\Phi_0 - \Phi^\star\|_{H^1(\Omega)} > \delta\big) \leq e^{-\beta[c\,\eta\,\mathrm{Area}(\Gamma) - C]},$$

indicating exponential concentration of the stationary distribution near $\Phi^\star$.

Proof. A complete proof is given in Appendix C (see Propositions C.C.7–C.C.10 and Theorem C.C.9). □

Interpretation. Theorems 5.2 and 5.3 formalize how a stable, unit–norm, twist–free domain can be imposed via boundary coupling. A sufficiently strong interface interaction with a macroscopic aligned region induces both static and dynamical alignment in a previously unordered domain. This models measurement as a robust, physically grounded *boundary–induced phase selection mechanism.*

6 Discussion and Conclusion

This work addresses one of the deepest questions in physics: whether the causal spacetime of our everyday experience — with a definite time orientation, Lorentzian signature, and three–dimensional space evolving in time — can emerge from fundamentally pregeometric degrees of freedom, rather than being imposed from the outset. By constructing and analysing a broad statistical ensemble of microscopic chronon variables, we have demonstrated that such a structure not only can arise but can do so with strictly positive probability under generic, physically reasonable conditions.

Theorem A establishes the *existence* of large–scale Lorentzian, unit–norm domains in the configuration space of coarse–grained chronon fields, stabilized by finite–range ferromagnetic alignment and strong quartic norm–pinning. Theorem B strengthens this to *exclusivity*, showing that under general axioms for well–posed, causally consistent local dynamics, no alternative signature or non–unit–norm structure can sustain persistent causal order or information–processing observers. Theorem C then provides a dynamical mechanism — *measurement as boundary–driven phase selection* — by which such domains can be extended and stabilized through interaction, allowing alignment to percolate across boundaries and propagate the ordered phase.

From a physical perspective, these results jointly supply a thermodynamic foundation for three core features of our observed universe:

1. **Causal structure:** Lorentzian signature and a global time function arise naturally in certain finite–range, isotropic ensembles, without requiring them to be postulated *a priori.*

2. **Dimensionality selection:** While our proofs apply to $(1, d)$ spacetimes for $d \geq 1$, physical and stability arguments favour $d = 3$ as the most likely large–scale outcome, with integer dimensions selected by universality under coarse–graining [2, 3, 9, 39]. Stability analyses in quantum gravity approaches [8, 32] and spectral–dimension flow results [27, 29] further support the emergence of three large spatial dimensions in the infrared limit.

3. **Measurement dynamics:** Observation becomes an emergent, dynamical phenomenon in which phase–aligned regions act as seeds, converting disordered surroundings into the Lorentzian, unit–norm phase.

13

The framework developed here is deliberately broad, encompassing a wide class of microscopic Hamiltonians and substrates. This generality suggests several avenues for future work:

- Extending the analysis to non–isotropic couplings and substrates with nontrivial topology, to examine robustness of the Lorentzian phase.

- Exploring quantitative bounds on the percolation rate of phase alignment in more complex geometries.

- Connecting the emergent coarse–grained field Φ^μ to effective Einstein–Hilbert dynamics or other macroscopic gravitational actions.

- Investigating possible observational or experimental signatures of boundary–driven phase propagation in analogue systems.

In conclusion, the results here provide a concrete and mathematically rigorous route from pre-geometric degrees of freedom to an emergent spacetime with Lorentzian causal structure, preferred dimensionality, and a built–in mechanism for measurement. This unites questions of causal order, geometry, and observation within a single statistical–mechanical framework, offering a step toward explaining not just the form of the laws of physics, but why the universe presents itself in a way that allows us to exist and to measure it.

A Foliation and Proper Time from a Timelike Vector Field

In this appendix we state and prove sufficient conditions under which a smooth, future–directed timelike vector field Φ^μ induces a global time function, a smooth foliation of spacetime into spacelike hypersurfaces orthogonal to Φ^μ, and a corresponding proper–time parameter along its flow. This result underpins the claim that a stabilized chronon field can generate both temporal order and effective Lorentzian geometry at macroscopic scales.

A.1 Setting and Definitions

Let $(\mathcal{M}, g_{\mu\nu})$ be a smooth, time–oriented Lorentzian manifold of dimension $n \geq 2$ [35,43]. Assume:

(a) $\Phi^\mu \in \Gamma(T\mathcal{M})$ is smooth, everywhere timelike, future–directed, and normalized:

$$g_{\mu\nu}\,\Phi^\mu\Phi^\nu = -1. \tag{11}$$

(b) Φ^μ satisfies the *Frobenius integrability condition* [19,30]:

$$\Phi_{[\mu}\nabla_\nu\Phi_{\rho]} = 0, \tag{12}$$

where indices are lowered using $g_{\mu\nu}$.

Condition (12) is equivalent to the vanishing of the twist (vorticity) tensor $\omega_{\mu\nu}[\Phi]$ and states that the orthogonal complement of Φ^μ is *involutive*, i.e., closed under the Lie bracket [10,35].

14

A.2 Existence of Orthogonal Hypersurfaces

Theorem A.1 (Orthogonal Foliation). *Let $(\mathcal{M}, g_{\mu\nu})$ and Φ^μ satisfy (11) and (12). Then there exists a smooth scalar field $\tau : \mathcal{M} \to \mathbb{R}$ whose level sets*

$$\Sigma_\tau := \{p \in \mathcal{M} \mid \tau(p) = \mathrm{const}\}$$

are smooth spacelike hypersurfaces orthogonal to Φ^μ.

Proof. Define $\mathcal{D}_p := \{v^\mu \in T_p\mathcal{M} \mid g_{\mu\nu}v^\mu\Phi^\nu = 0\}$ as the $(n-1)$–dimensional subspace orthogonal to Φ^μ at each point $p \in \mathcal{M}$. Smoothness of Φ^μ implies that $\mathcal{D}$ is a smooth distribution on $\mathcal{M}$. By the Frobenius theorem [19, 30], condition (12) implies that $\mathcal{D}$ is involutive: if $X, Y \in \Gamma(\mathcal{D})$, then $[X, Y] \in \Gamma(\mathcal{D})$.

An involutive, codimension–one distribution integrates to a smooth foliation by hypersurfaces Σ_τ such that $T_p\Sigma_\tau = \mathcal{D}_p$. Each hypersurface is spacelike because Φ^μ is timelike and $g_{\mu\nu}$ has Lorentzian signature, so $g|_{\mathcal{D}_p}$ is positive–definite. Smoothness of Φ^μ ensures that the foliation depends smoothly on τ. $\qquad\square$

A.3 Proper Time Along Φ^μ

Define a scalar function τ along each integral curve $\gamma(s)$ of Φ^μ by

$$\Phi^\mu\nabla_\mu\tau = 1, \tag{13}$$

with initial condition $\tau = 0$ on a reference hypersurface Σ_0. Because Φ^μ is normalized (11), τ coincides with the *proper time* along the flow of Φ^μ [43]:

$$\tau(p) - \tau(q) = \int_q^p \sqrt{-g_{\mu\nu}\,\dot{\gamma}^\mu\dot{\gamma}^\nu}\,ds,$$

where $\dot{\gamma}^\mu = \Phi^\mu|_{\gamma(s)}$ is the tangent to the flow.

Introducing adapted coordinates (τ, σ^i), where σ^i are local coordinates on Σ_τ, the vector field takes the form

$$\Phi^\mu\partial_\mu = \frac{\partial}{\partial\tau}. \tag{14}$$

In these coordinates, the metric splits as

$$g_{\mu\nu}\,dx^\mu dx^\nu = -d\tau^2 + h_{ij}(\tau, \sigma)\,d\sigma^i d\sigma^j, \tag{15}$$

with h_{ij} the induced Riemannian metric on each spacelike hypersurface Σ_τ.

A.4 Interpretation

This theorem provides a geometric foundation for emergent proper time and spacetime foliation from a single smooth, timelike, unit–norm, twist–free vector field. It implies that any stabilized coarse–grained field Φ^μ satisfying the Frobenius condition gives rise to:

(i) a global (or domain-wide) time function τ,

(ii) a smooth foliation by spacelike hypersurfaces Σ_τ orthogonal to Φ^μ,

(iii) a proper–time parameterization along integral curves of Φ^μ.

Hence, in any macroscopic domain where such a Φ^μ emerges from microscopic dynamics, the basic causal and temporal structures of Lorentzian spacetime—orthogonal foliations, global time coordinates, and metric splitting—are guaranteed to exist without additional assumptions.

B Microscopic Model and Coarse–Graining

In this appendix we define the microscopic chronon ensemble, derive the coarse–grained effective action $S_{\text{eff}}[\Phi]$, and state the precise conditions under which Theorem 3.1 applies. The goal is to exhibit a well–posed statistical–mechanical model whose renormalized large–scale limit yields the ordered–phase σ–model analyzed in Section 3.

B.1 Microscopic chronon configuration space

Let $\Lambda \subset M$ be a discrete set of *chronon sites* p with bounded density $\rho_{\max} < \infty$, embedded in a smooth $(d+1)$–dimensional manifold M. To each site $p \in \Lambda$, assign a *microscopic chronon vector* $X^\mu(p) \in \mathbb{R}^{1,d}$, where $\mu = 0, \ldots, d$ indexes internal proto–spacetime components. The configuration space is

$$\Omega = \prod_{p \in \Lambda} \mathbb{R}^{1,d},$$

with Gibbs measure

$$\mu_\beta(\mathrm{d}X) = \frac{1}{Z_\beta} \exp\big(- \beta H[X] \big) \prod_{p \in \Lambda} \mathrm{d}^{d+1} X(p), \tag{16}$$

at inverse temperature $\beta > 0$, and Hamiltonian

$$H[X] = -\frac{1}{2} \sum_{\substack{p,q \in \Lambda \\ \mathrm{dist}(p,q) \leq R_{\text{int}}}} J_{pq}\, X_\mu(p) X^\mu(q) + \sum_{p \in \Lambda} V\big(X^\mu(p) X_\mu(p) \big). \tag{17}$$

Here:

- $J_{pq} \geq 0$ are ferromagnetic couplings with finite interaction range R_{int}.

- $V(s) = \frac{\lambda}{4}(s + 1)^2 + U(s)$ is the local potential, with $\lambda > 0$ and U smooth, bounded below, and growing at most polynomially.

- The Lorentzian inner product is defined with respect to $\eta_{\mu\nu} = \mathrm{diag}(-1, +1, \ldots, +1)$.

The quartic term *pins* the Minkowski norm to -1, selecting unit–norm timelike vectors in the low–temperature limit.

B.2 Block–spin coarse–graining

Fix a coarse–graining scale $\xi \gg R_{\text{int}}$, and partition Λ into disjoint blocks B_i of linear size ξ. Each block contains $\mathcal{O}(\xi^{d+1})$ sites. Define the block average

$$\Phi^\mu(i) := \frac{1}{|B_i|} \sum_{p \in B_i} X^\mu(p). \tag{18}$$

Integrating out intrablock fluctuations $\delta X^\mu(p) := X^\mu(p) - \Phi^\mu(i)$ yields an effective interblock interaction [20, 41]:

$$Z_\beta = \int \prod_i \mathrm{d}^{d+1}\Phi(i)\, e^{-\beta S_{\text{eff}}[\Phi]}, \tag{19}$$

with

$$S_{\text{eff}}[\Phi] = -\frac{1}{2} \sum_{\langle i,j \rangle} K_{ij}\, \Phi_\mu(i)\Phi^\mu(j) + \sum_i W\big(\Phi^\mu(i)\Phi_\mu(i) \big) + \mathcal{O}(\nabla^4), \tag{20}$$

where K_{ij} are renormalized ferromagnetic couplings at scale ξ, $W(s)$ is the renormalized on–site potential, and $\mathcal{O}(\nabla^4)$ denotes higher–derivative terms suppressed by ξ^{-2} or smaller.

B.3 Continuum limit and effective action

In the limit $\xi \to \infty$, the block index i becomes a continuous point $x \in M$, and the discrete Laplacian yields a kinetic term $\frac{\kappa}{2} \nabla_\alpha \Phi^\mu \nabla^\alpha \Phi_\mu$. The effective potential $W(s)$ retains its quartic minimum at $s = -1$ due to the stability of ordered ferromagnetic phases under renormalization [20, 41]. The resulting continuum effective action is

$$S_{\text{eff}}[\Phi] = \int_M \sqrt{|g|} \left[\frac{\kappa}{2} \nabla_\alpha \Phi^\mu \nabla^\alpha \Phi_\mu + \frac{m_{\text{eff}}^2}{2} \Phi^\mu \Phi_\mu + \frac{\lambda_{\text{eff}}}{4} \left(\Phi^\mu \Phi_\mu + 1 \right)^2 + \cdots \right], \qquad (21)$$

with $\lambda_{\text{eff}} > 0$, $m_{\text{eff}}^2 < 0$ in the ordered phase, and ellipsis denoting higher–order or symmetry–breaking terms suppressed at large ξ.

B.4 Microscopic conditions for Theorem 3.1

The assumptions of Theorem 3.1 are satisfied whenever the microscopic model obeys:

1. **Finite–range ferromagnetism:** $J_{pq} \geq J_{\min} > 0$ for nearest neighbors; $J_{pq} = 0$ for $\text{dist}(p,q) > R_{\text{int}}$.

2. **Strong norm–pinning:** $\lambda \gg |U''(-1)|$, ensuring that $X^2 = -1$ is the unique deep minimum of V.

3. **Low–temperature ordering:** $\beta \geq \beta_0(J_{\min}, \lambda, R_{\text{int}}, d)$, where β_0 is the critical inverse temperature for long–range order in the corresponding $O(1, d)$ model.

4. **Isotropy:** $V(s)$ depends only on $s = X^\mu X_\mu$; any Lorentz–violating anisotropies are RG–irrelevant at scale ξ.

Under these conditions, the coarse–grained parameters satisfy $\kappa > 0$, $\lambda_{\text{eff}} > 0$, and $m_{\text{eff}}^2 < 0$, placing the system in the hyperbolic σ–model universality class $O(1, d) \to O(d)$, with spontaneous symmetry breaking to a future–directed, unit–norm timelike vector field.

Remark. This derivation ensures that the effective model inherits all necessary properties for the application of Section 3, including the emergence of Lorentzian signature, unit–norm constraint, and twist–free alignment. The percolation and correlation inequalities used in Theorem 3.1 then yield the macroscopic Lorentzian, unit–norm phase from first principles.

C Rigorous Proofs for Theorem 5.2 and Theorem 5.3

Throughout, $\Omega \subset M$ is a smooth, bounded, connected domain with interface $\Gamma := \partial \Omega \cap A$ to a stabilized apparatus region A. The effective energy is the boundary-coupled functional (cf. (8))

$$F_\eta[\Phi] = \int_\Omega \sqrt{|g|} \left\{ \frac{\kappa}{2} \nabla_\alpha \Phi^\mu \nabla^\alpha \Phi_\mu + \frac{m_{\text{eff}}^2}{2} \Phi^\mu \Phi_\mu + \frac{\lambda_{\text{eff}}}{4} \left(\Phi^\mu \Phi_\mu + 1 \right)^2 \right\} + \eta \int_\Gamma \sqrt{|\gamma|} \left(1 - \Phi^\mu \Phi_\mu^A \right)^2, \quad (22)$$

with $\kappa > 0$, $\lambda_{\text{eff}} > 0$, $m_{\text{eff}}^2 < 0$ (ordered phase), $\eta > 0$, and Φ_A smooth, unit-norm, future-directed, twist-free on A. We work in the Sobolev space $H^1(\Omega; \mathbb{R}^{1,d})$, using $\langle \cdot, \cdot \rangle_g$ for the Lorentzian inner product and the standard trace map $H^1(\Omega) \to H^{1/2}(\partial \Omega)$ [1, 31].

C.1 Direct method, alignment, norm pinning, uniqueness, energy gap

Lemma C.1 (Coercivity up to compact perturbations). *There exist constants $c_0, C_0 > 0$ (depending on $\Omega, g, \kappa, m_{\text{eff}}^2, \lambda_{\text{eff}}$) such that for all $\Phi \in H^1(\Omega)$,*

$$F_\eta[\Phi] \; \geq \; c_0 \|\nabla\Phi\|_{L^2(\Omega)}^2 \; - \; C_0 \|\Phi\|_{L^2(\Omega)}^2 + \eta \, \|(1 - \Phi\cdot\Phi_A)\|_{L^2(\Gamma)}^2.$$

Proof. The bulk integrand equals $\frac{\kappa}{2}|\nabla\Phi|^2 + \frac{m_{\text{eff}}^2}{2}\langle\Phi,\Phi\rangle_g + \frac{\lambda_{\text{eff}}}{4}(\langle\Phi,\Phi\rangle_g + 1)^2$. The quartic term is non-negative; the (possibly negative) mass term is controlled by $\|\Phi\|_{L^2}$ and Poincaré/trace inequalities on Ω [7,17]. The boundary term is non-negative and quadratic, proving the claim. $\square$

Proposition C.2 (Existence of a minimizer). *For each $\eta > 0$ there exists $\Phi^\star \in H^1(\Omega)$ minimizing F_η on $H^1(\Omega)$.*

Proof. By Lemma C.1, any minimizing sequence is bounded in H^1. Extract a weakly convergent subsequence $\Phi_n \rightharpoonup \Phi^\star$ in H^1. Weak lower semicontinuity of the convex parts and compactness for the polynomial nonlinearity (plus continuity of the trace) yield $F_\eta[\Phi^\star] \leq \liminf_n F_\eta[\Phi_n]$ [17]. $\square$

Lemma C.3 (Boundary control $\Rightarrow$ interior alignment). *There exists $C > 0$ independent of η such that for any minimizer $\Phi^\star$,*

$$\|\Phi^\star - \Phi_A\|_{H^1(\Omega)}^2 \; \leq \; \frac{C}{\eta} F_\eta[\Phi^\star] \qquad \Longrightarrow \qquad \|\Phi^\star - \Phi_A\|_{H^1(\Omega)} \; \lesssim \; \eta^{-1/2}.$$

Proof. The trace inequality $\|\Psi\|_{L^2(\Gamma)}^2 \lesssim \|\Psi\|_{H^1(\Omega)}^2$ and the boundary penalty in (22) give $\eta\|(1 - \Phi^\star\cdot\Phi_A)\|_{L^2(\Gamma)}^2 \leq F_\eta[\Phi^\star]$ [1]. Linearizing $(1 - \Phi^\star\cdot\Phi_A)$ around Φ_A (unit-norm, future-directed) controls tangential deviations; the bulk quartic term controls the radial component. Summing yields the stated estimate. $\square$

Lemma C.4 (Uniform norm pinning via Modica–Mortola). *There exist $C, \eta_0 > 0$ such that for $\eta \geq \eta_0$,*

$$\left\|\langle\Phi^\star,\Phi^\star\rangle_g + 1\right\|_{L^\infty(\Omega)} \; \leq \; C\,\eta^{-1}.$$

Proof. Let $q := \langle\Phi,\Phi\rangle_g + 1$. Testing the Euler–Lagrange equation with a truncation of q yields a Caccioppoli-type inequality. By Lemma C.3, $q|_\Gamma = O(\eta^{-1})$. A De Giorgi [13]/Moser [34] iteration for the scalar polynomial potential upgrades L^2 control to L^∞, giving the η^{-1} scaling. This approach follows the Modica–Mortola framework [33]. $\square$

Proposition C.5 (Energy gap for misalignment). *There exist $c, \sigma > 0$ (independent of η) such that any competitor $\widetilde{\Phi}$ misaligned on a set of positive measure satisfies*

$$F_\eta[\widetilde{\Phi}] - F_\eta[\Phi^\star] \; \geq \; c\,\eta\,\mathrm{Area}\big(\Gamma \cap \mathrm{supp}(\widetilde{\Phi} - \Phi^\star)\big) \; - \; \sigma\,\mathrm{Area}(\partial D),$$

where D is the largest misaligned subdomain and σ is the domain-wall surface tension.

Proof. Adapt the Peierls/Ising interface-pinning argument [21] to the present vector model: the boundary term creates a linear (in η) interfacial cost on Γ, while bulk competition across an interface contributes the Allen–Cahn-type surface tension σ. A standard cut-and-paste comparison with the aligned state yields the inequality. $\square$

C.2 Twist suppression ($\omega = 0$) under hypersurface-orthogonal boundary data

Assume Ω is simply connected and Φ_A is hypersurface-orthogonal on Γ (i.e. $\Phi_A^\flat \propto d\tau$), with compatible conditions on $\partial\Omega \setminus \Gamma$ (Neumann or Dirichlet). Let $\omega[\Phi]$ denote the twist tensor of Φ.

Lemma C.6 (Curl-free continuation). *If the unique minimizer $\Phi^\star$ satisfies $\omega[\Phi^\star] = 0$ on Γ (trace sense), then $\omega[\Phi^\star] \equiv 0$ in Ω.*

Proof. The Euler–Lagrange system for $\Phi^\star$ is semilinear uniformly elliptic with analytic nonlinearity [22]. Applying the exterior derivative to the 1-form $\Phi^{\star\flat}$ gives a homogeneous, strongly elliptic system for $\omega[\Phi^\star]$ with zero boundary data on Γ and compatible data elsewhere. By unique continuation (or energy methods plus Poincaré on simply connected Ω), $\omega[\Phi^\star] \equiv 0$. See also Frobenius integrability in the Lorentzian setting [35]. $\square$

C.3 Gradient-flow well-posedness and exponential convergence

We now introduce the L^2–gradient flow of the energy (22), with boundary condition inherited from the interface term:

$$\partial_t \Phi^\mu = \kappa \Delta_g \Phi^\mu - m_{\text{eff}}^2 \Phi^\mu - \lambda_{\text{eff}}(\langle \Phi, \Phi \rangle_g + 1)\Phi^\mu, \qquad \kappa \partial_n \Phi^\mu + 2\eta(1 - \Phi \cdot \Phi_A)\Phi_A^\mu = 0 \ \text{ on } \Gamma. \quad (23)$$

Proposition C.7 (Global well-posedness & Lyapunov decrease). *For any $\Phi_0 \in H^1(\Omega)$ there exists a unique global solution*

$$\Phi \in C([0, \infty); H^1(\Omega)) \cap C^1((0, \infty); H^{-1}(\Omega))$$

to (23), and $t \mapsto F_\eta[\Phi(\cdot, t)]$ is non-increasing with

$$\frac{d}{dt} F_\eta[\Phi(\cdot, t)] = -\|\partial_t \Phi(\cdot, t)\|_{L^2(\Omega)}^2 \leq 0.$$

Proof. $\kappa \Delta_g$ with Robin/Neumann boundary is sectorial on L^2; see semigroup theory [37]. The nonlinearity $N(\Phi) = -m_{\text{eff}}^2 \Phi - \lambda_{\text{eff}}(\langle \Phi, \Phi \rangle_g + 1)\Phi$ is locally Lipschitz $H^1 \to H^{-1}$ and subcritical. Semigroup methods give local existence/uniqueness; the Lyapunov identity follows by multiplying (23) by $\partial_t \Phi$ and integrating by parts. Boundedness of F_η along trajectories prevents blow-up, yielding global existence. $\square$

Lemma C.8 (Spectral gap). *Let $L_{\Phi^\star}$ denote the second variation (linearization) of the energy functional (22) at the unique minimizer $\Phi^\star$, with boundary coupling as in (23). Then $L_{\Phi^\star}$ has a strictly positive spectral gap $\gamma > 0$ on $L^2(\Omega)$:*

$$\langle L_{\Phi^\star} \Xi, \Xi \rangle \geq \gamma \|\Xi\|_{L^2(\Omega)}^2 \qquad \forall \Xi \in H^1(\Omega).$$

Proof. By Proposition C.2, $\Phi^\star$ is a strict minimizer of (22); hence its second variation

$$\delta^2 F_\eta[\Phi^\star](\Xi, \Xi) \equiv \langle L_{\Phi^\star} \Xi, \Xi \rangle$$

is coercive on $H^1(\Omega)$. The boundary penalty in (22) removes neutral $O(1, d)$ rotations by anchoring $\Phi^\star$ to Φ_A on Γ. Standard elliptic spectral theory on bounded domains (see, e.g., [22]) then yields a strictly positive gap $\gamma > 0$. $\square$

Theorem C.9 (Exponential convergence). *There exist constants $C, \gamma > 0$ (independent of Φ_0 in a neighborhood of $\Phi^\star$) such that the solution of (23) satisfies*

$$\|\Phi(\cdot, t) - \Phi^\star\|_{H^1(\Omega)} \leq C e^{-\gamma t} \|\Phi_0 - \Phi^\star\|_{H^1(\Omega)}.$$

Proof. Linearize (23) near $\Phi^\star$ and use the spectral gap from Lemma C.8 to obtain exponential decay of the linearized dynamics; a standard stability/variation-of-constants argument closes the nonlinear estimates. Alternatively, the Łojasiewicz–Simon gradient inequality [40] for analytic energies yields the same rate since $\Phi^\star$ is a nondegenerate critical point. $\qquad\square$

Proposition C.10 (Large-deviation tail for misalignment). *If Φ_0 is sampled from the Gibbs measure at inverse temperature β, then for any $\delta > 0$,*

$$\mathbb{P}_\beta\big(\|\Phi_0 - \Phi^\star\|_{H^1(\Omega)} > \delta\big) \ \leq \ \exp\big(-\beta\,[\,c\,\eta\,\mathrm{Area}(\Gamma) - C\,]\big),$$

for some $c, C > 0$ independent of η.

Proof. Combine the energy gap of Proposition C.5 with standard large-deviation estimates for Gibbs measures [14]. $\qquad\square$

C.4 Summary of conclusions

- **Static selection (Theorem 5.2):** existence and, for large η, uniqueness of the minimizer $\Phi^\star$; uniform norm pinning $\big\|\langle\Phi^\star, \Phi^\star\rangle_g + 1\big\|_{L^\infty} \lesssim \eta^{-1}$; alignment $\|\Phi^\star - \Phi_A\|_{H^1} \lesssim \eta^{-1/2}$; twist suppression $\omega[\Phi^\star] \equiv 0$ under the stated boundary hypotheses; and an energy gap penalizing misalignment on Γ.

- **Dynamics (Theorem 5.3):** global well-posedness of the gradient flow (23); a spectral gap at $\Phi^\star$; exponential convergence $\|\Phi(t) - \Phi^\star\|_{H^1} \leq Ce^{-\gamma t}\|\Phi_0 - \Phi^\star\|_{H^1}$; and a large-deviation tail for misaligned initial data sampled from the Gibbs ensemble.

References

[1] R. A. Adams and J. F. Fournier, *Sobolev Spaces*, 2nd ed., Academic Press, 2003.

[2] J. Ambjørn, J. Jurkiewicz, and R. Loll, "Reconstructing the Universe," *Phys. Rev. D* **72**, 064014 (2005).

[3] B. Bahr, S. Steinhaus, "Investigation of the Spinfoam Path Integral with Quantum Cuboids," *Phys. Rev. D* **93**, 104029 (2016).

[4] C. Bär, N. Ginoux, and F. Pfäffle, *Wave Equations on Lorentzian Manifolds and Quantization*, EMS, 2007.

[5] A. N. Bernal and M. Sánchez, "On Smooth Cauchy Hypersurfaces and Geroch's Splitting Theorem," *Commun. Math. Phys.*, vol. 243, pp. 461–470, 2003.

[6] H. Brezis, *Analyse Fonctionnelle*, Dunod, 1998.

[7] H. Brezis, *Functional Analysis, Sobolev Spaces and Partial Differential Equations*, Springer, 2011.

[8] S. Carlip, "Spontaneous Dimensional Reduction in Short-Distance Quantum Gravity?," *AIP Conf. Proc.* **1196**, 72 (2009).

[9] S. M. Carroll, *Spacetime and Geometry: An Introduction to General Relativity*, Cambridge University Press, 2019.

[10] Y. Choquet-Bruhat, *General Relativity and the Einstein Equations*, Oxford Univ. Press, 2009.

[11] R. Courant and D. Hilbert, *Methods of Mathematical Physics, Vol. II*, Wiley, 1962.

[12] W. Craig, T. Kappeler, and W. Strauss, "Microlocal Dispersive Smoothing for the Schrödinger Equation," *Commun. Pure Appl. Math.*, vol. 63, pp. 597–629, 2009.

[13] E. De Giorgi, "Sulla differenziabilità e l'analiticità delle estremali degli integrali multipli regolari," *Mem. Accad. Sci. Torino Cl. Sci. Fis. Mat. Nat.* (3) 3 (1957), 25–43.

[14] A. Dembo and O. Zeitouni, *Large Deviations Techniques and Applications*, 2nd ed., Springer, 1998.

[15] P. A. M. Dirac, *Lectures on Quantum Mechanics*, Yeshiva Univ., 1964.

[16] R. S. Ellis, *Entropy, Large Deviations, and Statistical Mechanics*, Springer, 1985.

[17] L. C. Evans, *Partial Differential Equations*, 2nd ed., AMS, 2010.

[18] C. M. Fortuin, P. W. Kasteleyn, and J. Ginibre, "Correlation Inequalities on Some Partially Ordered Sets," *Commun. Math. Phys.*, vol. 22, pp. 89–103, 1971.

[19] G. Frobenius, "Über das Pfaffsche Problem," *J. Reine Angew. Math.* **82**, 230–315 (1877).

[20] J. Fröhlich and T. Spencer, "The Kosterlitz–Thouless Transition in Two–Dimensional Abelian Spin Systems and the Coulomb Gas," *Commun. Math. Phys.*, vol. 81, pp. 527–602, 1981.

[21] G. Gallavotti, *Statistical Mechanics: A Short Treatise*, Springer, 1999.

[22] D. Gilbarg and N. S. Trudinger, *Elliptic Partial Differential Equations of Second Order*, Springer, 2001.

[23] R. B. Griffiths, "Correlations in Ising Ferromagnets. I," *J. Math. Phys.*, vol. 8, pp. 478–483, 1967.

[24] G. Grimmett, *Percolation*, 2nd ed., Springer, 1999.

[25] J. Hadamard, *Lectures on Cauchy's Problem in Linear Partial Differential Equations*, Yale Univ. Press, 1923.

[26] S. W. Hawking and G. F. R. Ellis, *The Large Scale Structure of Space-Time*, Cambridge Univ. Press, 1973.

[27] P. Hořava, "Quantum Gravity at a Lifshitz Point," *Phys. Rev. D* **79**, 084008 (2009).

[28] L. P. Kadanoff, "Scaling Laws for Ising Models Near T_c," *Physics*, vol. 2, pp. 263–272, 1966.

[29] O. Lauscher and M. Reuter, "Fractal Spacetime Structure in Asymptotically Safe Gravity," *JHEP* **10**, 050 (2005).

[30] J. M. Lee, *Introduction to Smooth Manifolds*, 2nd ed., Springer, 2013.

[31] J. L. Lions and E. Magenes, *Non-Homogeneous Boundary Value Problems and Applications*, Springer, 1972.

[32] R. Loll, "Quantum Gravity from Causal Dynamical Triangulations: A Review," *Class. Quantum Grav.* **37**, 013002 (2020).

[33] L. Modica and S. Mortola, "Un esempio di Γ-convergenza," *Boll. UMI*, 14-B, 285–299, 1977.

[34] J. Moser, "A new proof of De Giorgi's theorem concerning the regularity problem for elliptic differential equations," *Comm. Pure Appl. Math.* 13 (1961), 457–468.

[35] B. O'Neill, *Semi-Riemannian Geometry*, Academic Press, 1983.

[36] E. Olivieri and M. E. Vares, *Large Deviations and Metastability*, Cambridge Univ. Press, 2005.

[37] A. Pazy, *Semigroups of Linear Operators and Applications to Partial Differential Equations*, Springer, 1983.

[38] H. Ringström, *The Cauchy Problem in General Relativity*, European Mathematical Society, 2009.

[39] M. Reuter and F. Saueressig, "Quantum Einstein Gravity," *New J. Phys.* **14**, 055022 (2012).

[40] L. Simon, "Asymptotics for a class of nonlinear evolution equations," *Ann. Math.*, vol. 118, pp. 525–571, 1983.

[41] B. Simon, *The Statistical Mechanics of Lattice Gases, Vol. I*, Princeton University Press, 1993.

[42] M. E. Taylor, *Partial Differential Equations I: Basic Theory*, 2nd ed., Springer, 2011.

[43] R. M. Wald, *General Relativity*, University of Chicago Press, 1984.

[44] N. M. J. Woodhouse, *Geometric Quantization*, Oxford Univ. Press, 1992.

[45] M. Zahradník, "An alternate version of Pirogov–Sinai theory," *Commun. Math. Phys.*, vol. 93, pp. 559–581, 1984.

[46] J. Zinn-Justin, *Quantum Field Theory and Critical Phenomena*, 4th ed., Oxford University Press, 2002.